Ain Shams Engineering Journal 9 (2018) 2587–2598

Contents lists available at ScienceDirect

Ain Shams Engineering Journal

journal homepage: www.sciencedirect.com

Engineering Physics and Mathematics

Making conditionally negative definite radial basis function interpolation well-conditioned by adding cardinal basis functions

Saeed Kazem [a], Edmund A. Chadwick [b], Ali Hatam [a,*]

[a] Department of Applied Mathematics, Faculty of Mathematics and Computer Science, Amirkabir University of Technology, No. 424, Hafez Ave., 15914 Tehran, Iran
[b] School of Computing, Science and Engineering, University of Salford, Salford M5 4WT, UK

ARTICLE INFO

Article history:
Received 17 September 2016
Revised 27 January 2017
Accepted 12 March 2017
Available online 12 October 2017

AMS subject classifications:
65M20
65M06

Keywords:
Radial basis functions
Cardinal functions
Multiquadrics (MQ)

ABSTRACT

A class of basis functions so called well-conditioned RBF (WRBFs) has been introduced. This basis has been manipulated by adding cardinal functions to the conditionally negative definite RBFs of order 1, such as Multiquadric functions $\sqrt{1+(\epsilon r)^2}$ (MQ) and $\log(1+(\epsilon r)^2)$ (LOG). The condition number of the interpolation matrix arising from this basis is of $\mathcal{O}(N)$, where N is the number of center nodes. This order is independent of shape parameter and therefore applying this basis functions would recover the ill–posed linear system associated with the order 1 conditionally negative definite RBFs interpolation.

1. Introduction

Historically, RBFs interpolation were first proposed by Roland Hardy in 1968 [1]. This method allows scattered data to be easily used in computations. Franke [2] then deduced that the RBFs interpolations were accurate, comparing well with other available methods. Kansa [3,4] first used RBFs to solve differential equations (DEs) as an approximation to the solution. However, in recent years RBFs have been extensively researched in a wider range of analysis and applications [5–20].

In the case of Multiquadric (MQ) $\phi(r)=\sqrt{1+(\epsilon r)^2}$ and (LOG) $\phi(r)=\log(1+(\epsilon r)^2)$, the interpolation matrices have one positive eigenvalue and the rest are distinctly negative [21]. Madych and Nelson [22] show that interpolation with MQ is exponentially convergent from the Native space. But the interpolation matrix of negative definite RBFs of order 1 are ill–conditioned. The condition number of the matrix exponentially grows as the number of nodes increases, meanwhile the shape parameter decreases and this often prevents the RBF method from attaining reasonable spectral accuracy [23]. For smooth functions, a reasonable accuracy for a given number of nodes may be achieved when the shape parameter is small, but the instability associated with small shape parameters leads to an unreliable approximation. Fornberg and Wright [24], Fornberg and Piret [25], Fornberg and Larsson [26] developed some algorithms to overcome the instability arising from small shape parameter. Also Larsson et al. [27] introduced the RBF-QR algorithm which is computationally stable for flat RBF interpolation, and it is easier to implement rather than Contour-Padé and also it can be implemented for a large number of nodes. A stabilization process to improve the accuracy of the positive definite kernel, such as the Tikhonov regularization, has been investigated by Wendland and Rieger [28] and Sarra [29]. Also there exist some classical techniques which allow us to change the original space basis by using the reproducing kernel of the associated native space for conditionally positive definite functions to get an interpolation matrix with condition number depending only on the number of data points [30, chp. 34]. This approach was suggested by Beatson, Light and Billings [31], using the result of [32].

In this work, a new family of functions involving the conditionally negative definite RBFs of order 1 and also cardinal functions, has been introduced. The result of this basis is an interpolation

* Corresponding author.
E-mail addresses: saeedkazem@aut.ac.ir (S. Kazem), e.a.chadwick@salford.ac.uk (E.A. Chadwick), alihatam@aut.ac.ir (A. Hatam).
Peer review under responsibility of Ain Shams University.

Production and hosting by Elsevier

http://dx.doi.org/10.1016/j.asej.2017.03.013
2090-4479/

matrix with condition number of $\mathcal{O}(N)$ and independent of small shape parameter.

2. Conditionally negative definite RBFs of order 1

Let f be a real function defined on a domain in $\mathbb{R}^d$, if $\{\mathbf{x}_i, i = 1, 2, \ldots, N\}$ is a set of nodes belong to its domain, then an RBFs approximation $\tilde{f}_N$ to f would be defined as follows:

$$f(\mathbf{x}) \approx \tilde{f}_N(\mathbf{x}) = \sum_{i=1}^{N} a_i \phi_i(\mathbf{x}) = \Phi^T(\mathbf{x})\mathbf{a}, \tag{1}$$

where $\phi_i(\mathbf{x}) = \phi(\|\mathbf{x} - \mathbf{x}_i\|_2), \Phi^T(\mathbf{x}) = [\phi_1(\mathbf{x}), \phi_2(\mathbf{x}), \ldots, \phi_N(\mathbf{x})]$ and $\mathbf{a} = [a_1, a_2, \ldots, a_N]^T$. $\mathbf{a}$ will be determined through the linear system $\mathbf{\Phi a} = \mathbf{f}$, where, $\mathbf{f} = [f(\mathbf{x}_1), f(\mathbf{x}_2), \ldots, f(\mathbf{x}_N)]^T$ and $\mathbf{\Phi} = (\phi_i(\mathbf{x}_j))_{N\times N}$ is so called interpolation matrix. Powell [21] shows that in the cases of Multiquadric (MQ) and (LOG), the interpolation matrices have one positive eigenvalue and the rest are distinctly negative, therefore we may sort them out as follows

$$\lambda_1 > 0 > \lambda_2 > \ldots > \lambda_N.$$

This kind of RBFs are known as conditionally negative definite RBFs of order 1.

Narcowich and Ward [33] present some upper bounds for condition numbers, $\kappa(\mathbf{\Phi}) = \|\mathbf{\Phi}\|_2\|\mathbf{\Phi}^{-1}\|_2$, of MQ and LOG interpolation matrices as follows:

$$\begin{array}{ll} d = 2 & d = 3 \\ 5.95G(q,D)e^{3/p} & 8.55G(q,D)e^{4/p} \quad \textbf{MQ}, \end{array} \tag{2}$$

$$0.99\frac{H(q,D)}{K_0\left(\frac{3}{p}\right)} \qquad 2.14\frac{H(q,D)}{K_0\left(\frac{4}{p}\right)} \quad \textbf{LOG}, \tag{3}$$

where,

$$G(q,D) = \frac{\sqrt{1+D^2}}{p}\left(\frac{D+2\epsilon q}{2\epsilon q}\right)^3,$$

$$H(q,D) = \log(1+D^2)\left(\frac{D+2\epsilon q}{2\epsilon q}\right)^3, p = \frac{\epsilon^2 q^2}{1+\sqrt{1+\epsilon^2 q^2}},$$

$K_0(.)$ is the zero order modified Bessel function of the second kind, $q = \frac{1}{2}\min_{i\neq j}\|\mathbf{x}_j - \mathbf{x}_i\|_2$ and $D = \max_{i,j}\|\mathbf{x}_i - \mathbf{x}_j\|_2$.

The following theorem provides bounds for eigenvalues of interpolation matrices arising from MQ and LOG basis.

Theorem 1. *Let $\lambda_1 > 0 > \lambda_2 > \ldots > \lambda_N$ be all eigenvalues of the matrix $\mathbf{\Phi}$ subordinate to Multiquadric and Logarithmic bases, then $\kappa(\mathbf{\Phi}) = \lambda_1/|\lambda_2|$ and also there hold,*

$$\begin{array}{ll} \lambda_1 < 1 + (N-1)\sqrt{1+\epsilon^2 D^2}, & \lambda_N > 1 - (N-1)\sqrt{1+\epsilon^2 D^2}, \quad \textbf{MQ}, \\ \lambda_1 < (N-1)\log(1+\epsilon^2 D^2), & \lambda_N > (1-N)\log(1+\epsilon^2 D^2), \quad \textbf{LOG}. \end{array}$$

Proof. For matrix $\mathbf{\Phi}$, we have $trace(\mathbf{\Phi}) = \sum_{i=1}^{N}\phi_i(\mathbf{x}_i) = \sum_{i=1}^{N}\lambda_i = \lambda_1 - \sum_{i=2}^{N}|\lambda_i|$, and therefore

$$\lambda_1 = \sum_{i=1}^{N}\phi_i(\mathbf{x}_i) + \sum_{i=2}^{N}|\lambda_i|.$$

Since in cases MQ and LOG, $\phi_i(\mathbf{x}_i)$ is equal to 1 and 0 respectively, then

$$\lambda_1 = N + \sum_{i=2}^{N}|\lambda_i|, \quad \textbf{MQ}, \qquad \& \qquad \lambda_1 = \sum_{i=2}^{N}|\lambda_i|, \quad \textbf{LOG}.$$

Obviously $\lambda_1 > |\lambda_i|, i = 2, \ldots, N$, and since $\mathbf{\Phi}$ is symmetric and non-singular, we have $\|\mathbf{\Phi}\|_2 = \lambda_1$ and $\|\mathbf{\Phi}^{-1}\|_2 = |1/\lambda_2|$, hence $\kappa(\mathbf{\Phi}) = \lambda_1/|\lambda_2|$. According to Gershgorin circle theorem, for each $i = 1, \ldots, N$ there holds

$$-\sum_{\substack{j=1\\ j\neq i}}^{N}\phi_i(\mathbf{x}_j) \leqslant \lambda - \phi_i(\mathbf{x}_i) \leqslant \sum_{\substack{j=1\\ j\neq i}}^{N}\phi_i(\mathbf{x}_j),$$

applying to functions MQ and LOG yield

$$\begin{array}{ll} 1 - \sum\limits_{j=1, j\neq i}^{N}\sqrt{1+\epsilon^2\|\mathbf{x}_j - \mathbf{x}_i\|_2^2} \leqslant \lambda \leqslant 1 + \sum\limits_{j=1, j\neq i}^{N}\sqrt{1+\epsilon^2\|\mathbf{x}_j - \mathbf{x}_i\|_2^2}, & \textbf{MQ}, \\ -\sum\limits_{j=1, j\neq i}^{N}\log\left(1+\epsilon^2\|\mathbf{x}_j - \mathbf{x}_i\|_2^2\right) \leqslant \lambda \leqslant \sum\limits_{j=1, j\neq i}^{N}\log\left(1+\epsilon^2\|\mathbf{x}_j - \mathbf{x}_i\|_2^2\right), & \textbf{LOG}. \end{array}$$ □

Theorem 1 implies that the biggest eigenvalue of $\mathbf{\Phi}$ increases linearly, in number of nodes and shape parameter. But according to (2) and (3), $\kappa(\mathbf{\Phi})$ increases exponentially in terms of N and ϵ. Therefore an increase in N or decrease in ϵ leads to an exponential decrease in $|\lambda_2|$ (Figs. 1 and 2).

3. Well-conditioned RBF basis

Here we wish to define another approximation f_N to f based on WRBFs, as follows:

$$f(\mathbf{x}) \approx f_N(\mathbf{x}) = \sum_{i=1}^{N} b_i \psi_i(\mathbf{x}), \tag{4}$$

where

$$\psi_i(\mathbf{x}) = \phi(\|\mathbf{x} - \mathbf{x_i}\|_2) - pC_i(\mathbf{x}), \quad p > 0, \quad C_i(\mathbf{x}_j) = \delta_{ij}, \quad i,j = 1, 2, \ldots, N, \tag{5}$$

$\phi(\|.\|_2)$ is the conditionally negative definite RBFs of order 1, $C_i(\mathbf{x})$ is a cardinal function and δ_{ij} denotes the Kronecker delta. We call the parameter p, *effective parameter*. Any changes on this parameter will directly affect function interpolation. Unknown vector $\mathbf{b} = [b_1, b_2, \ldots, b_N]^T$ is determined through the linear system $\Psi\mathbf{b} = \mathbf{f}$, where the interpolation matrix $\Psi = (\psi_i(\mathbf{x}_j))_{N\times N}$ is also equal to $\Psi = \mathbf{\Phi} - pI$. Obviously if $p < \lambda_1$ then the matrix Ψ is nonsingular and conditionally negative definite of order 1.

Theorem 2. *Let $\lambda_1 > 0 > \lambda_2 > \ldots > \lambda_N$ be all eigenvalues of the matrix $\mathbf{\Phi}$ subordinate to Multiquadric and Logarithmic bases, if $\Psi = \mathbf{\Phi} - pI$, for a $p < \lambda_1$, then*

$$\kappa(\Psi) < \mathcal{M}\max\left\{\frac{1}{\lambda_1 - p}, \frac{1}{p - \lambda_2}\right\}, \tag{6}$$

where $\mathcal{M} = |1-p| + (N-1)\sqrt{1+\epsilon^2 D^2}$ for MQ basis and $\mathcal{M} = p + (N-1)\log(1+\epsilon^2 D^2)$ for LOG basis.

Proof. As well as $\mathbf{\Phi}$, the matrix Ψ is also symmetric and then $\|\Psi\|_2 = \max_i|\lambda_i(\Psi)|$.

Applying the Gershgorin circle theorem to Ψ, yields

$$|\lambda| - |\phi_i(\mathbf{x}_i) - p| \leqslant |\lambda + p - \phi_i(\mathbf{x}_i)| \leqslant \sum_{j=1, j\neq i}^{N}\phi_i(\mathbf{x}_j),$$

hence

$$\begin{array}{ll} \|\Psi\|_2 < |1-p| + (N-1)\sqrt{1+\epsilon^2 D^2}, & \textbf{MQ}, \\ \|\Psi\|_2 < p + (N-1)\log(1+\epsilon^2 D^2), & \textbf{LOG}. \end{array}$$

Also

$$\|\Psi^{-1}\|_2 = \max_i|\lambda_i(\Psi^{-1})| = \max_i\left|\frac{1}{\lambda_i - p}\right| = \max\left\{\frac{1}{\lambda_1 - p}, \frac{1}{p - \lambda_2}\right\}. \tag{7}$$

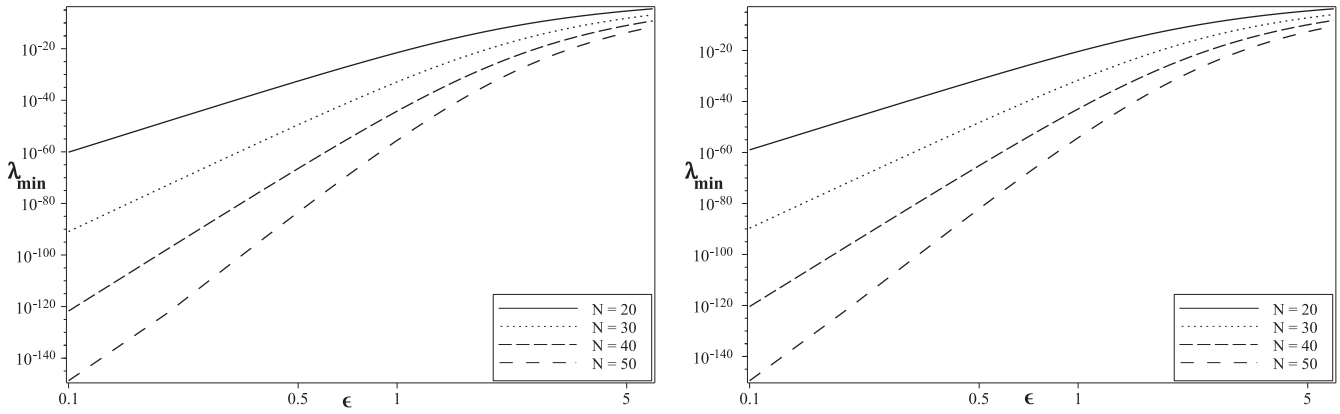

Fig. 1. $\lambda_{min} = |\lambda_2|$ of interpolation matrix on $[0, 1]$ with uniform grid for various number of nodes N, MQ (*left*), LOG (*right*).

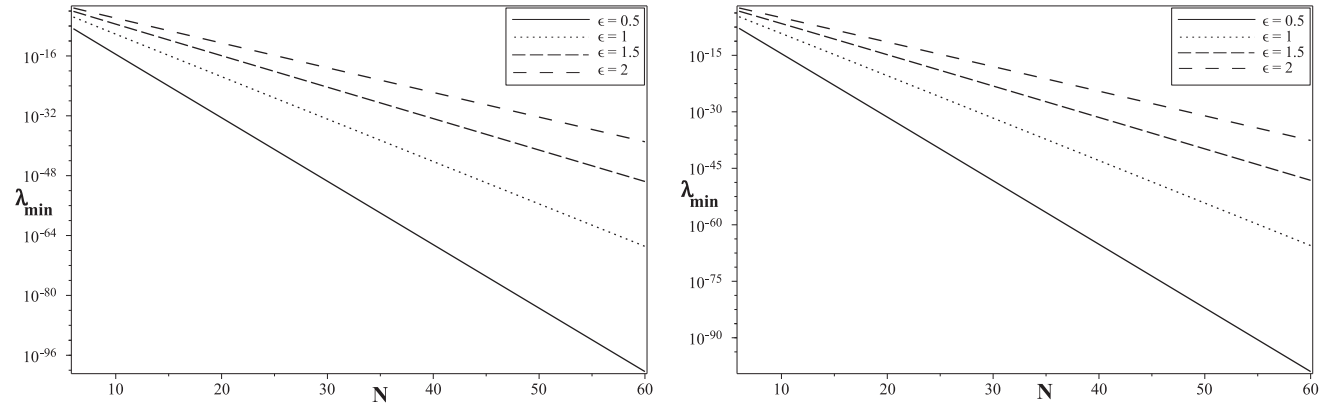

Fig. 2. $\lambda_{min} = |\lambda_2|$ of interpolation matrix on $[0, 1]$ with uniform grid for different shape parameters ϵ, MQ (*left*), LOG (*right*).

Accordingly, we deduce

$$\kappa(\Psi) = \|\Psi\|_2 \max\left\{\frac{1}{\lambda_1 - p}, \frac{1}{p - \lambda_2}\right\},$$

and the proof is now complete.

Corollary. *For positive $p < (\lambda_1 + \lambda_2)/2$, there hold*

$$\kappa(\Psi) < \frac{|1-p| + (N-1)\sqrt{1+\epsilon^2 D^2}}{p}, \qquad \textbf{MQ},$$

$$\kappa(\Psi) < 1 + \frac{(N-1)\log(1+\epsilon^2 D^2)}{p}, \qquad \textbf{LOG}.$$

These bounds show that the order of condition number of the WRBFs interpolation matrix is $\mathcal{O}(N)$. Using these bases also removes any influences of the small shape parameter in ill-conditioning of the interpolation matrix. In Table 1, $\kappa(\Psi)$ (denoted by $\kappa(p)$) has been computed for MQ and LOG–WRBFs interpolations with uniform grid on $[0, 1]$ and $\epsilon = 0.1$. This Table shows that the growth of the condition number of WRBFs interpolation matrix is linear when N increases. Also in this Table the values of λ_1, λ_2, $\mathcal{M}$ and the values of $U(p)$ the upper bound of $\kappa(\Psi)$ mentioned in (6), are provided. The condition number of Ψ in domain $[0, 1]^2$ and $[0, 1]^3$ with random nodes for various values N and ϵ have been displayed in Figs. 3 and 4. Fig. 5 shows the influences of shape parameters in condition number of matrix Ψ, accordingly the small shape parameter does not increase $\kappa(\Psi)$ arising from pure RBF basis.

We now compare the results of our proposed basis in terms of the condition number and also RMS errors with the well conditioned basis which is constructed by using the reproducing kernels of thin plate splines in $\mathbb{R}^2$ [30,31].

Table 2 indicates a comparison between the condition number of the interpolation matrix for standard MQ and LOG and also the WRBFs bases with the reproducing kernels of thin plate splines [31] obtained by uniform grids on the unit square $[0, 1]^2$. In this Table, the number of nodes and the separation distance h change from one row to the next.

In Table 3, the number of nodes is fixed but the separation distance h varies from one row to the next. This Table shows that decrease in the separation distance does not cause an increase in the condition number of the new bases against the standard ones.

In Table 4, the RMS errors for interpolating Franke's function via different bases are reported. According to this Table, increasing the scaling parameter has no significantly effect in accuracy on the new bases, in spite of it being shown in this Table that the accuracy of MQ–WRBF interpolation improves as the scale parameter a decreases.

3.1. Gaussian cardinal functions

Let us to define the Quasi-Cardinal Gaussian RBF as follows

$$Q_i(\mathbf{x}) = \mathrm{e}^{-\frac{\alpha^2}{d_i^2}\|\mathbf{x}-\mathbf{x_i}\|_2^2}, d_i = \min_{j\in\{1,2,\ldots,N\}-\{i\}} \|\mathbf{x}_j - \mathbf{x_i}\|_2, i = 1, \ldots, N, \quad \alpha > 0,$$

obviously, $Q_i(\mathbf{x}_i) = 1$ and $Q_i(\mathbf{x}_j) \leqslant \mathrm{e}^{-\alpha^2}$. For large enough α, these type of functions generate near diagonal interpolation matrices.

Table 1
The values of condition number Ψ (denoted by $\kappa(p)$) for MQ and LOG–WRBFs interpolations with uniform grid on $[0,1]$ and $\epsilon = 0.1$ and also the values of λ_1, λ_2, $\mathcal{M}$ and the value of $U(p)$ upper bound of $\kappa(\Psi)$ in Theorem 2.

$N-1 \rightarrow$	4	8	16	32	64	128	256
MQ–WRBF:							
$\kappa(10^{-6})$	5.01e+06	9.01e+06	1.70e+07	3.30e+07	6.51e+07	1.29e+08	2.57e+08
$\kappa(10^{-8})$	5.00e+08	9.02e+08	1.71e+09	3.32e+09	6.54e+09	1.30e+10	2.57e+10
$\kappa(10^{-10})$	4.90e+10	9.01e+10	1.70e+11	3.30e+11	6.51e+11	1.29e+12	2.58e+12
λ_1	5.006	9.009	17.016	33.029	65.056	129.110	257.216
$-\lambda_2$	2.17e−12	9.14e−17	4.39e−17	3.03e−17	3.31e−17	1.10e−17	6.28e−18
$\mathcal{M}$	5.020	9.040	17.080	33.160	65.319	129.638	258.277
$U(10^{-6})$	5.02e+06	9.04e+06	1.71e+07	3.32e+07	6.53e+07	1.30e+08	2.58e+08
$U(10^{-8})$	5.02e+08	9.04e+08	1.71e+009	3.32e+09	6.53e+09	1.30e+10	2.58e+10
$U(10^{-10})$	4.91e+10	9.04e+10	1.71e+11	3.32e+11	6.53e+11	1.30e+12	2.58e+12
LOG–WRBF:							
$\kappa(10^{-6})$	14346	21779	37165	68219	1.30e+05	2.55e+05	5.04e+05
$\kappa(10^{-8})$	1.43e+06	2.18e+06	3.72e+06	6.88e+06	1.32e+07	2.59e+07	5.04e+07
$\kappa(10^{-10})$	1.23e+08	2.17e+08	3.71e+08	6.82e+08	1.30e+09	2.55e+09	5.05e+09
λ_1	0.014	0.022	0.037	0.068	0.130	0.255	0.504
$-\lambda_2$	1.64e−11	1.84e−17	1.12e−18	2.81e−19	1.00e−19	1.01e−20	2.28e−21
$\mathcal{M}$	0.040	0.080	0.159	0.318	0.637	1.274	2.547
$U(10^{-6})$	39801	79603	1.59e+05	3.18e+05	6.37e+05	1.27e+06	2.54e+06
$U(10^{-8})$	3.97e+06	7.96e+06	1.59e+07	3.18e+07	6.37e+07	1.27e+08	2.55e+08
$U(10^{-10})$	3.42e+08	7.96e+08	1.59e+09	3.18e+09	6.37e+09	1.27e+10	2.55e+10

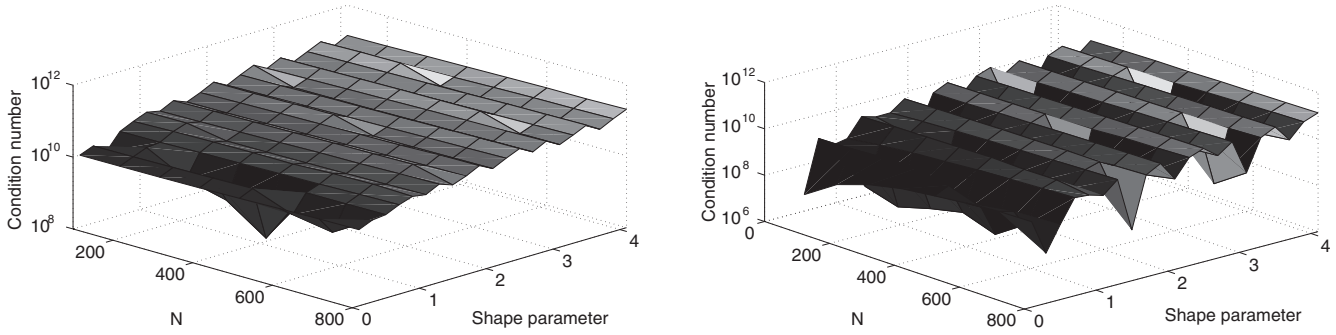

Fig. 3. $\kappa(\Psi)$ when MQ and LOG–WRBFs interpolate random nodes on $[0,1]^2$ with $p = 10^{-8}$, MQ (*left*), LOG (*right*).

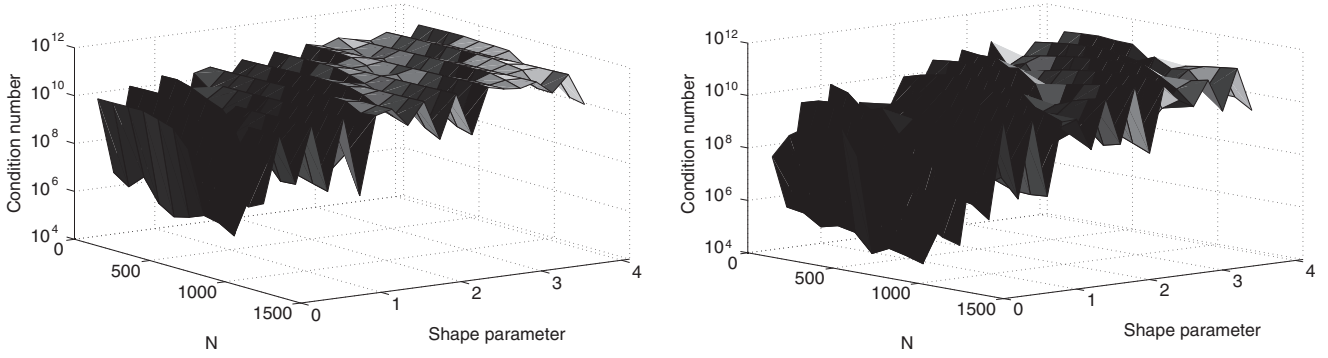

Fig. 4. $\kappa(\Psi)$ when MQ and LOG–WRBFs interpolate random nodes on $[0,1]^3$ with $p = 10^{-8}$, MQ (*left*), LOG (*right*).

The cardinal functions using the Quasi–Cardinal Gaussian RBFs can be simply constructed by

$$C(\mathbf{x}) = Q^{-1}Q(\mathbf{x}), \qquad Q(\mathbf{x}) = [Q_1(\mathbf{x}), \ldots, Q_N(\mathbf{x})]^T,$$
$$Q_{ij} = \phi\left(\frac{\alpha}{d_i}\|\mathbf{x_j} - \mathbf{x_i}\|_2\right).$$

Q is the interpolation matrix due to Quasi–cardinal Gaussian RBF which is close to Identity matrix and hence Q^{-1} is easy to compute.

Fig. 6 shows the condition numbers of matrix Q for three values α, and different numbers of random nodes in $[0,1]^2$, according to these results the matrix is well-conditioned for $\alpha \geqslant 1$.

3.2. Convergence of WRBF

Now we are going to prove that the convergence of WRBF basis behaves the same as RBF interpolation when p tends to zero. For this purpose, let us denote $\hat{f}_N(\mathbf{x}) = \sum_{i=1}^{N} f_i C_i(\mathbf{x})$ as Cardinal

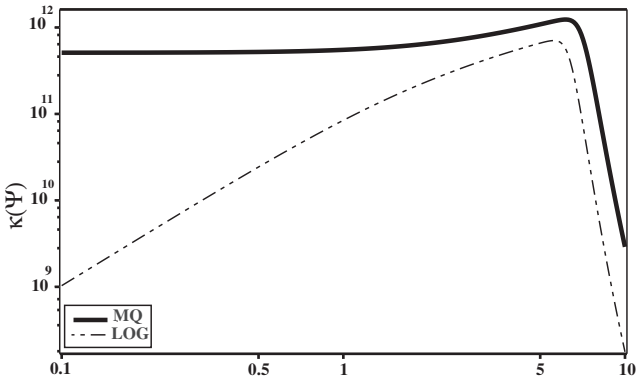

Fig. 5. $\kappa(\Psi)$ when MQ and LOG–WRBFs interpolate uniform grid on $[0,1]$ with $N=50$ and $p=10^{-10}$.

approximation to the function f, ($f_i = f(\mathbf{x}_i)$) as well as in (1) we considered $\tilde{f}_N(\mathbf{x})$ as an RBF approximation to f, then we will have the error bounds for these approximations as follows

$$\|f-\tilde{f}_N\| \leqslant \tilde{k}(f)\tilde{u}_N, \qquad \|f-\hat{f}_N\| \leqslant \hat{k}(f)\hat{u}_N, \tag{8}$$

where $\|.\|$ denotes the maximum norm, $\tilde{k}(f)$ and $\hat{k}(f)$ are positive constants depend on $f, \tilde{u}_N$ and $\hat{u}_N$ are positive sequences independent of f and depend on the number of nodes or fill distance. We may consider $\tilde{u}_N = \exp\left(\frac{-c}{h_{\chi,\Omega}}\right)$, $\tilde{k}(f) = |f|_{\mathcal{N}_\Phi(\Omega)}$ and also for Cardinal basis constructed by Gaussian basis $\hat{k}(f) = \|f\|_{\mathcal{N}_\Phi(\Omega)}$, where $|.|_{\mathcal{N}_\Phi(\Omega)}$ and $\|.\|_{\mathcal{N}_\Phi(\Omega)}$ are semi-norm and norm in the Native space $\mathcal{N}_\Phi(\Omega)$ respectively, $h_{\chi,\Omega}$ is the fill distance and c is a positive constant (Theorem 15.1 [30]).

Table 2
Condition numbers for different thin plate spline bases $[E]$ and MQ and LOG–WRBFs on $[0,1]^2$ with $\epsilon=0.1$, $p=10^{-6}$ and increasing number of points and varying separation distance h.

h	standard TPS	reproducing kernel TPS	homogeneous TPS	MQ	LOG	MQ–WRBF	LOG–WRBF
1/8	3.515800e+03	1.839030e+04	7.583833e+03	9.9693e+18	4.5784e+18	6.4137e+07	2.9708e+05
1/16	3.893850e+04	2.651373e+05	1.108581e+05	3.4772e+19	6.1499e+17	2.5648e+08	1.0509e+06
1/32	5.136252e+05	4.000679e+06	1.686431e+06	8.3443e+19	4.8160e+18	1.0258e+09	3.9519e+06
1/64	7.618277e+06	6.202918e+07	2.626402e+07	1.0740e+21	2.6430e+19	4.1031e+09	1.5325e+07

Table 3
Condition numbers for different thin plate spline bases $[E]$ and MQ and LOG–WRBFs on $[0,a]^2$ with $\epsilon=0.1$, $p=10^{-6}$ and fixed number of 25 points.

a	standard TPS	reproducing kernel TPS	homogeneous TPS	MQ	LOG	MQ–WRBF	LOG–WRBF
0.001	2.434883e+08	8.463509e+08	5.493771e+02	1.1931e+26	2.3630e+18	2.5000e+07	1.2285
0.01	2.436378e+06	8.464002e+06	5.493771e+02	3.7585e+23	8.9288e+16	2.5000e+07	12.5118
1	3.645782e+02	1.366035e+03	5.493771e+02	3.0852e+17	4.5910e+14	2.5062e+07	1.3448e+05
100	1.151990e+11	1.139634e+05	5.493771e+02	419.7601	88.8807	419.7590	88.8806
1000	3.548239e+15	1.138572e+07	5.493771e+02	161.9042	37.1090	161.9042	37.1090

Table 4
RMS errors for different thin plate spline bases $[C]$ and MQ and LOG–WRBFs on $[0,a]^2$ with $\epsilon=5$, $p=10^{-12}$ and fixed number of 25 points.

a	reproducing kernel TPS	homogeneous TPS	MQ	LOG	MQ–WRBF	LOG–WRBF
10^{-9}	NaN	2.969478e−02	NaN	NaN	2.5091e−11	4.03e−02
10^{-6}	2.970740e−02	2.969478e−02	4.9653e−11	6.3187e−06	4.2232e−10	1.14e−03
10^{-3}	2.969478e−02	2.969478e−02	1.8014e−09	1.3641e−10	9.7949e−10	1.24e−09
1	2.969478e−02	2.969478e−02	2.66e−02	2.79e−02	0.0266e−02	2.79e−02
10^3	2.969478e−02	2.969478e−02	6.79e−02	4.06e−02	0.0679e−02	4.06e−02
10^6	2.969218e−02	2.969478e−02	6.78e−02	3.47e−02	0.0678e−02	3.47e−02
10^9	1.207446e+03	2.969478e−02	6.78e−02	3.29e−02	0.0678e−02	3.29e−02

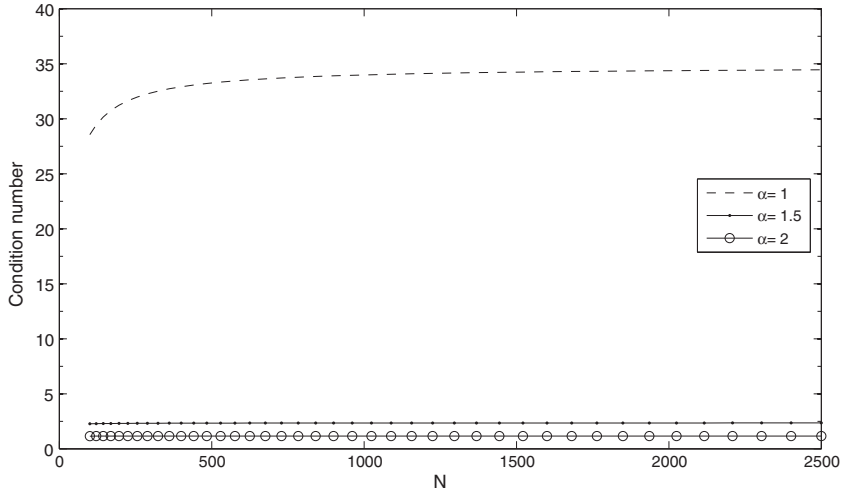

Fig. 6. The condition number of Q for $\alpha=1,\ 1.5$ and 2.

We now investigate the convergence of WRBF according to the error bounds (8). It should be noted that these error bounds are not only applicable for constructing Cardinal functions based on the Gaussian basis, but they can also be used for any Cardinal functions for which the error bounds are expressed by maximum norm.

Lemma 1. *Any cardinal function $C_i(\mathbf{x}), i = 1, 2, \ldots, N$ has an approximation $\widetilde{C}_i(\mathbf{x})$ in terms of radial basis functions $\phi_j(\mathbf{x})$ such that $\widetilde{C}_i(\mathbf{x}) = \mathbf{\Phi}_i^{-1}\Phi(\mathbf{x})$, where $\mathbf{\Phi}_i^{-1}$ denotes the i's row of matrix $\mathbf{\Phi}^{-1}$ [34].*

Proof. Define

$$\widetilde{C}_i(\mathbf{x}) = \sum_{j=1}^{N} v_{ij}\phi_j(\mathbf{x}) = \mathbf{v}_i^T\Phi(\mathbf{x}), \tag{9}$$

applying N collocation nodes $\mathbf{x}_j$, $j = 1, \ldots, N$ in (9) and using the cardinal property $\widetilde{C}_i(\mathbf{x}_j) = \delta_{ij}$ yields $\mathbf{e}_i^T = \mathbf{v}_i^T\mathbf{\Phi}$, $i = 1, 2, \ldots, N$, where $\mathbf{e}_i$ is the unit vector with all entries zero unless, one at i's place. Hence $\mathbf{v}_i^T = \mathbf{e}_i^T\mathbf{\Phi}^{-1}$ is the i's row of $\mathbf{\Phi}^{-1}$. □

Take $C(\mathbf{x}) = [C_1(\mathbf{x}), \ldots, C_N(\mathbf{x})]^T$, then Lemma 1 gives the following bound for $\widetilde{C}_i(\mathbf{x})$ as follows

$$\left\|C_i(\mathbf{x}) - \mathbf{\Phi}_i^{-1}\Phi(\mathbf{x})\right\| = \left\|C_i(\mathbf{x}) - \widetilde{C}_i(\mathbf{x})\right\| \leqslant \tilde{k}(C_i)\tilde{u}_N, \tag{10}$$

where $\tilde{k}(C_i)$ is a positive constant depends on C_i as well as has been explained for (8). Following theorem shows that f_N tends to f when $p \to 0$.

Theorem 3. *If f_N and $\tilde{f}_N$ are two approximations to f, due to WRBF and RBF bases, respectively, with $p < (\lambda_1 + \lambda_2)/2$, then there holds*

$$\|f - f_N\| < \tilde{k}(f)\tilde{u}_N + \tilde{k}_{max}\|\mathbf{f}\|_1\sqrt{N}\tilde{u}_N,$$

where $\tilde{k}_{max} = \max_i \tilde{k}(C_i)$.

Proof. From (1), (4) and (5) the following identities are obtained:

$\tilde{f}_N = \mathbf{a}^T\Phi(\mathbf{x})$, $f_N = \mathbf{b}^T\Psi(\mathbf{x}) = \mathbf{b}^T\Phi(\mathbf{x}) - p\mathbf{b}^TC(\mathbf{x})$, $\Psi = \mathbf{\Phi} - pI, \mathbf{b} = \Psi^{-1}\mathbf{f}$ and $\mathbf{a} = \mathbf{\Phi}^{-1}\mathbf{f}$.

Now we can write

$$\begin{aligned} f_N - \tilde{f}_N &= (\mathbf{b} - \mathbf{a})^T\Phi(\mathbf{x}) - p\mathbf{b}^TC(\mathbf{x}) \\ &= \mathbf{f}^T(\Psi^{-1} - \mathbf{\Phi}^{-1})\Phi(\mathbf{x}) - p\mathbf{f}^T\Psi^{-1}C(\mathbf{x}), \end{aligned}$$

substituting $\mathbf{b}^T = \mathbf{f}^T\Psi^{-1}$ and $\Psi = \mathbf{\Phi} - pI$ in recent result, yields

$$f_N - \tilde{f}_N = \mathbf{b}^T\left[(I - \Psi\mathbf{\Phi}^{-1})\Phi(\mathbf{x}) - pC(\mathbf{x})\right] = p\mathbf{b}^T\left[\mathbf{\Phi}^{-1}\Phi(\mathbf{x}) - C(\mathbf{x})\right],$$

and then

$$\begin{aligned} \|f_N - \tilde{f}_N\| &= p\left\|\mathbf{b}^T\left(C(\mathbf{x}) - \mathbf{\Phi}^{-1}\Phi(\mathbf{x})\right)\right\| \\ &\leqslant p\sum_{i=1}^{N}|b_i|\left\|C_i(\mathbf{x}) - \mathbf{\Phi}_i^{-1}\Phi(\mathbf{x})\right\| \leqslant \tilde{k}_{max}\tilde{u}_N\|p\mathbf{b}\|_1, \end{aligned} \tag{11}$$

using the matrix norm equivalence, yields

$$\|p\mathbf{b}\|_1 = \|p\Psi^{-1}\mathbf{f}\|_1 \leqslant \|p\Psi^{-1}\|_1\|\mathbf{f}\|_1 \leqslant \sqrt{N}\|p\Psi^{-1}\|_2\|\mathbf{f}\|_1.$$

Ψ^{-1} is symmetric and non-singular, recalling that λ_2 is negative, according to (7), we get

$$\|p\Psi^{-1}\|_2 = \frac{p}{p - \lambda_2} = \frac{p}{p + |\lambda_2|} < 1,$$

and therefore

$$\|f_N - \tilde{f}_N\| \leqslant \tilde{k}_{max}\sqrt{N}\|\mathbf{f}\|_1\tilde{u}_N.$$

Recent result together with (8) deduce

$$\begin{aligned} \|f - f_N\| = \left\|f - \tilde{f}_N + \tilde{f}_N - f_N\right\| &\leqslant \left\|f - \tilde{f}_N\right\| + \left\|\tilde{f}_N - f_N\right\| \\ &\leqslant \tilde{k}(f)\tilde{u}_N + \tilde{k}_{max}\sqrt{N}\|\mathbf{f}\|_1\tilde{u}_N, \end{aligned}$$

and now the proof is complete. □

Theorem 3 clarifies that the convergence of WRBF when p tends to zero is similar to RBF approximation. Following theorem (Thm. 4) asserts that the error of WRBF interpolation may be considered as a convex combination of the errors obtained by the RBF and the cardinal bases.

Theorem 4. *For the approximation f_N to f defined in (4), and $p < (\lambda_1 + \lambda_2)/2$, there holds*

$$\|f - f_N\| \leqslant \frac{\tilde{k}(f) + p\tilde{\alpha}}{1 + p}\tilde{u}_N + p\frac{\hat{k}(f) + \hat{\alpha}}{1 + p}\hat{u}_N, \tag{12}$$

where $\tilde{\alpha} = \sum_{i=1}^{N}|b_i|\tilde{k}(C_i)$ and $\hat{\alpha} = \sum_{i=1}^{N}|b_i|\hat{k}(\phi_i)$.

Proof.

$$\|f - f_N\| = \left\|f - \tilde{f}_N + \tilde{f}_N - f_N\right\| \leqslant \tilde{k}(f)\tilde{u}_N + \left\|f_N - \tilde{f}_N\right\|, \tag{13}$$

$$\|f - f_N\| = \left\|f - \hat{f}_N + \hat{f}_N - f_N\right\| \leqslant \hat{k}(f)\hat{u}_N + \left\|f_N - \hat{f}_N\right\|. \tag{14}$$

Multiplying both sides of Eq. (14) by p and adding to Eq. (13) yields

$$\begin{aligned} \|f - f_N\| \leqslant \frac{\tilde{k}(f)}{1 + p}\tilde{u}_N + p\frac{\hat{k}(f)}{1 + p}\hat{u}_N + \frac{1}{1 + p}\left\|f_N - \tilde{f}_N\right\| \\ + \frac{p}{1 + p}\left\|f_N - \hat{f}_N\right\|. \end{aligned} \tag{15}$$

In (11) we have

$$\left\|f_N - \tilde{f}_N\right\| \leqslant p\sum_{i=1}^{N}|b_i|\left\|C_i(\mathbf{x}) - \mathbf{\Phi}_i^{-1}\Phi(\mathbf{x})\right\|,$$

which together with (10) yield

$$\left\|f_N - \tilde{f}_N\right\| \leqslant p\sum_{i=1}^{N}|b_i|\tilde{k}(C_i)\tilde{u}_N. \tag{16}$$

Also, from (4) we have $\mathbf{f}^T = \mathbf{b}^T\Psi$, and then

$$\begin{aligned} f_N - \hat{f}_N &= \mathbf{b}^T\Phi(\mathbf{x}) - p\mathbf{b}^TC(\mathbf{x}) - \mathbf{f}^TC(\mathbf{x}) = \mathbf{b}^T\Phi(\mathbf{x}) - \mathbf{b}^T(pI + \Psi)C(\mathbf{x}) \\ &= \mathbf{b}^T(\Phi(\mathbf{x}) - \mathbf{\Phi}C(\mathbf{x})), \end{aligned}$$

therefore

$$\left\|f_N - \hat{f}_N\right\| = \left\|\mathbf{b}^T(\Phi(\mathbf{x}) - \mathbf{\Phi}C(\mathbf{x}))\right\| \leqslant \sum_{i=1}^{N}|b_i|\|\phi_i(\mathbf{x}) - \mathbf{\Phi}_iC(\mathbf{x})\|,$$

where $\mathbf{\Phi}_i$ denotes the i's row of $\mathbf{\Phi}$. Let $\hat{\phi}_i(\mathbf{x})$ be the Cardinal approximation to ϕ_i, then $\hat{\phi}_i(\mathbf{x}) = \mathbf{\Phi}_iC(\mathbf{x})$ and according to (8) we will have

$$\|\phi_i(\mathbf{x}) - \mathbf{\Phi}_iC(\mathbf{x})\| = \left\|\phi_i(\mathbf{x}) - \hat{\phi}_i(\mathbf{x})\right\| \leqslant \hat{k}(\phi_i)\hat{u}_N, \tag{17}$$

eventually

$$\left\|f_N - \hat{f}_N\right\| \leqslant \sum_{i=1}^{N}|b_i|\hat{k}(\phi_i)\hat{u}_N. \tag{18}$$

Applying (16) and (18) in (15) completes the proof. □

Another result from Theorem 4 states that when p tends to zero the function approximation f_N (WRBF approximation) approaches to the RBF approximation $\tilde{f}_N$ and according to inequality (15) the

convergence of WRBF becomes similar to the RBF approximation, same result will be obtained when p tends to infinity. Therefore the convergence of WRBF is same as the cardinal approximation.

Therefore the conditionally negative definite RBFs of order 1 such as MQ and LOG bases, which are exponentially accurate [35–37], are appropriate candidates to construct WRBF bases with small p. In this algorithm p needs to be:

(1) large enough to improve conditioning.
(2) small enough to provide fast convergence.

Such as Riley's algorithm [38], the practical suggestion for p is $p \approx 10^{-q+v}$, where q is desired precision, and $v = 2$ or 3 or bigger according to increasing in the number of nodes [32].

3.3. Test problems

Problem 1. Consider the second-order differential equation $u'' - \mu^2 u = 0, x \in [-1, 1]$, with exact solution $u = e^{\mu x}$. The maximum error obtained by the solutions of pure MQ, pure LOG and WRBF with $\mu = 0.1, 50$ and uniform grid for various shape parameters and $\epsilon = 0.2$ is displayed in Fig. 7.

Also Fig. 8 shows the error due to increasing in number of nodes without any changes in shape parameter. In practice these figures corroborate the Quasi–Cardinal–WRBF method with small effective parameter p works better than pure RBFs for this problem.

Problem 2. We now test the 2d Poisson equation with exact solutions

$u_1 = 105/(105 + x^2 + y^2)$ and $u_2 = y(1-y)x^3$

on $[0, 1]^2$ with Dirichlet boundary condition. 400 uniform grid, MQ, LOG and WRBFs, have been applied to this problem, the maximum errors corresponding to various shape parameters have been illustrated in Figs. 9 and 10.

Problem 3. Consider 3d Poisson equation with exact solutions

$v_1 = 135/(135 + x^2 + y^2 + z^2)$ and
$v_2 = (1/3\pi^2)\sin(\pi x)\sin(\pi y)\sin(\pi z)$

on $[0, 1]^3$ with Dirichlet boundary condition. 1000 uniform grid, MQ, LOG and WRBFs, have been applied to this problem. For various shape parameters the corresponding maximum errors have also been shown in Figs. 11 and 12. All Figs. 9–12 state that the Quas i–cardianl–WRBF method with small effective parameter p works better than pure RBFs for these particular problems.

3.3.1. A comparison with RBF-QR

To corroborate the stability and reliability of the proposed basis, we compare the errors using a stable evaluation method such as RBF-QR [26,27] and the WRBF basis to 2d Poisson equation with exact solutions

$w_1 = 1,\ w_2 = \exp(x + y)$ and $w_3 = \sin(5\pi x)\sin(5\pi y)$

on $[0, 1]^2$ with Dirichlet boundary conditions.

Fig. 13 shows the condition numbers and errors using RBF-QR method and the WRBF basis, as a function of N, with fixed shape parameter $\epsilon = 0.01$ and uniform grid, applied to Poisson equation with exact solution w_1. This figure verifies that the WRBF with

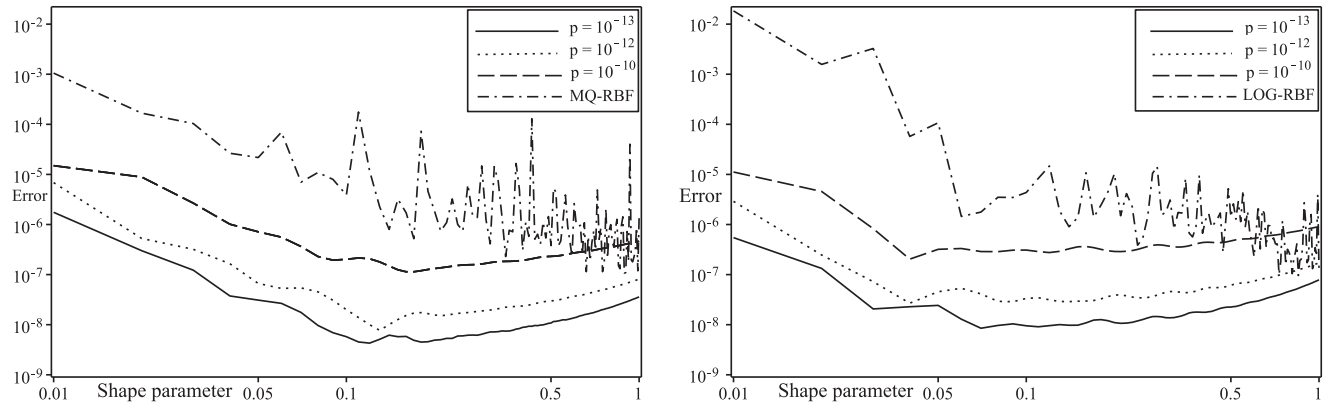

Fig. 7. The l_∞ error for solution of test 1, using 50 uniform grid for effective parameters $p = 10^{-10}, 10^{-12}, 10^{-13}$ with MQ (*left*) and LOG (*right*).

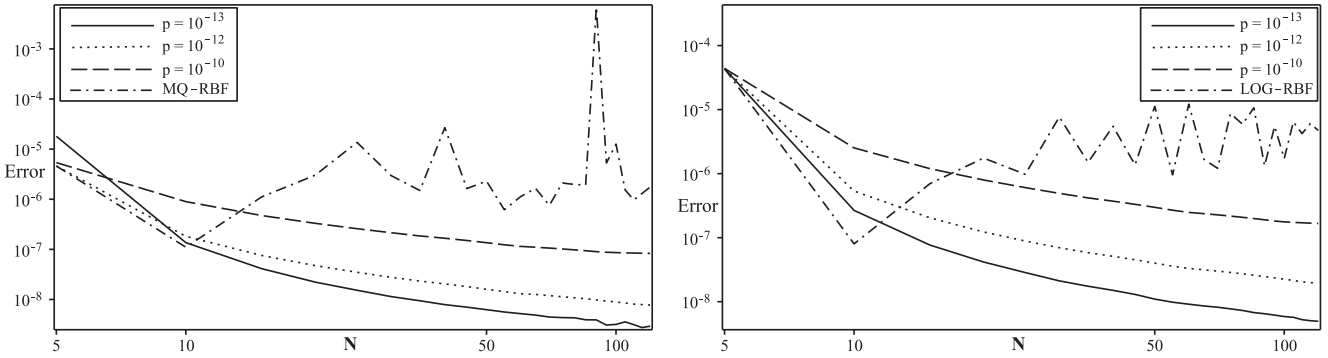

Fig. 8. The l_∞ error for solution of test 1, with $\epsilon = 0.2$ for MQ (*left*) and LOG (*right*).

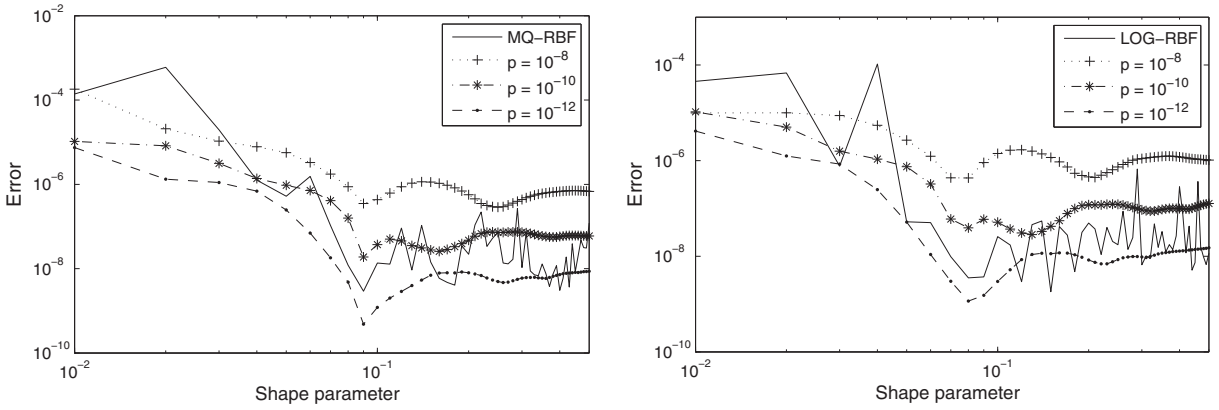

Fig. 9. The l_∞ error for solution of the 2d Poisson equation (u_1) using 400 uniform grid with MQ (*left*) and LOG (*right*).

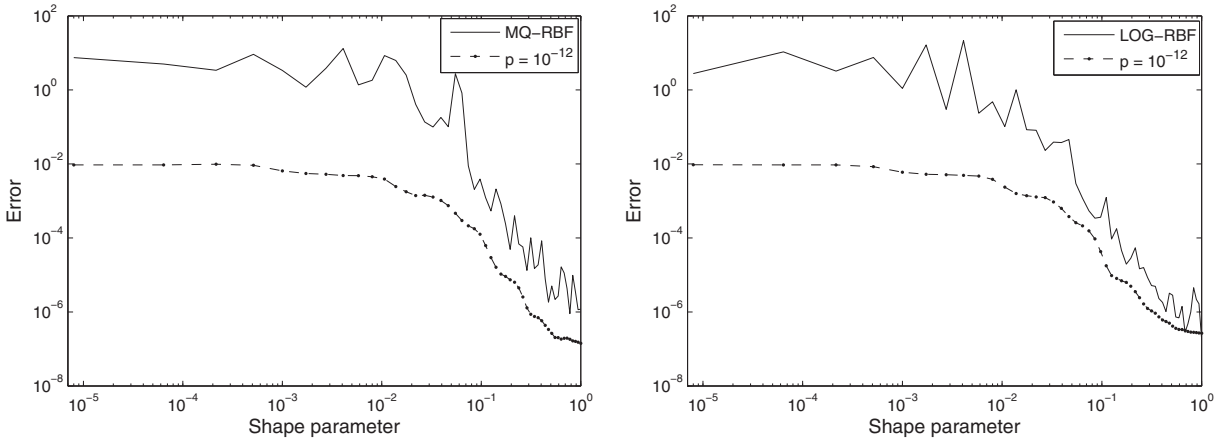

Fig. 10. The l_∞ error for solution of the 2d Poisson equation (u_2) using 400 uniform grid with MQ (*left*) and LOG (*right*).

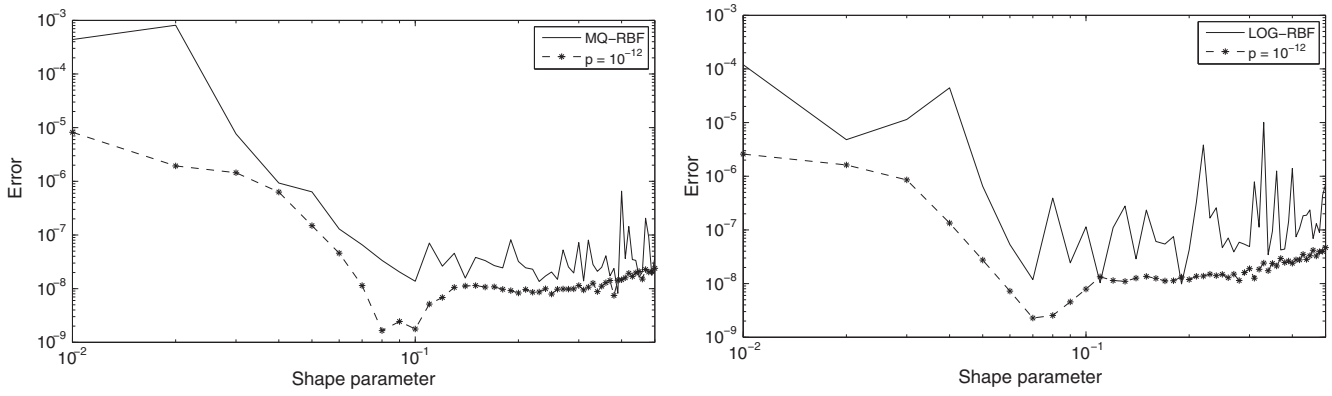

Fig. 11. The l_∞ error for solution of the 3d Poisson equation (v_1) using 1000 uniform grid with MQ (*left*) and LOG (*right*).

small shape parameter for solving the Poisson equation is stable for large numbers of nodes.

In Fig. 14, the RBF-QR method and the WRBF basis have been applied to Poisson equation with exact solution w_2, and shape parameter $\epsilon = 0.5$. Also this figure shows the condition numbers and maximum errors corresponding to different number of nodes.

Errors and condition numbers for solutions of Poisson equation with exact solution w_3, and shape parameters $\epsilon = 0.01,\ 0.5, 1$ and 1.5 corresponding to various number of nodes have been illustrated in Fig. 15. For this problem the reasonable solution was obtained for $\epsilon \geqslant 1$. We now apply a time dependent problem.

Problem 4. Consider the Caputo sense time-fractional diffusion equation [39]

$$\partial_t^\beta u(x,t) = \gamma u_{xx}(x,t) + f(x,t), \qquad x \in [0,1],\ t > 0,\ \beta \in (0,1], \tag{19}$$

and Dirichlet boundary condition with exact solution

$$u(x,t) = E_\beta(-t^\beta)g(x),$$

where $f(x,t) = -E_\beta(-t^\beta)(g(x) + \gamma g''(x))$.

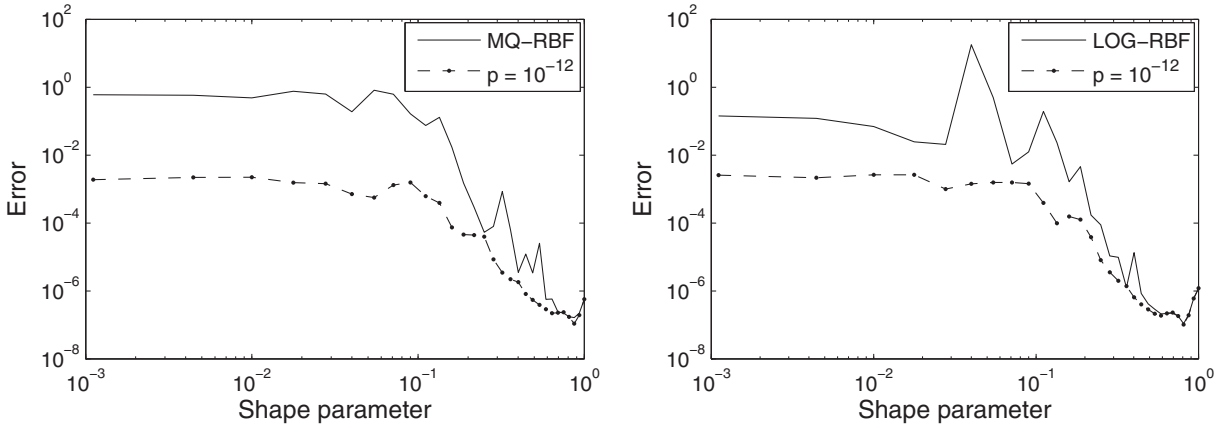

Fig. 12. The l_∞ error for solution of the 3d Poisson equation (v_2) using 1000 uniform grid with MQ (*left*) and LOG (*right*).

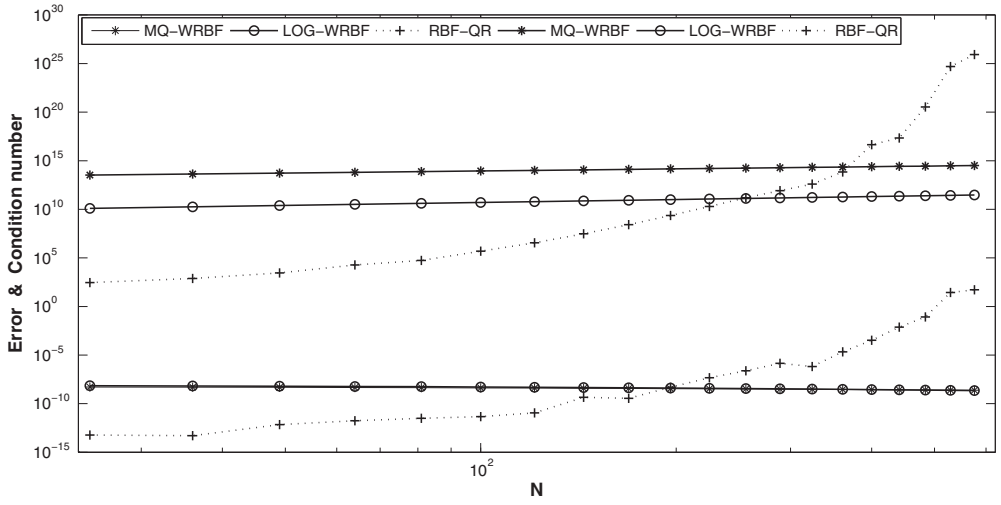

Fig. 13. The condition number and l_∞ error for solutions of 2d Poisson equation with exact solution 1, with RBF-QR method, MQ-WRBF and LOG-WRBF basis with $\epsilon = 0.01$ and $p = 10^{-12}$.

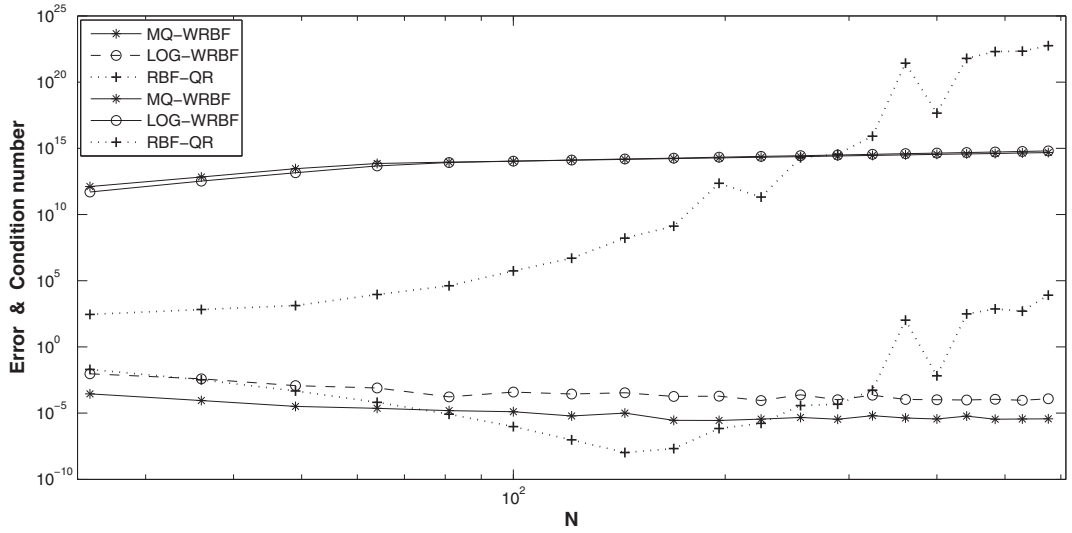

Fig. 14. The condition number and l_∞ error for solutions of 2d Poisson equation with exact solution w_2, with RBF-QR method, MQ-WRBF and LOG-WRBF basis with $\epsilon = 0.5$ and $p = 10^{-12}$.

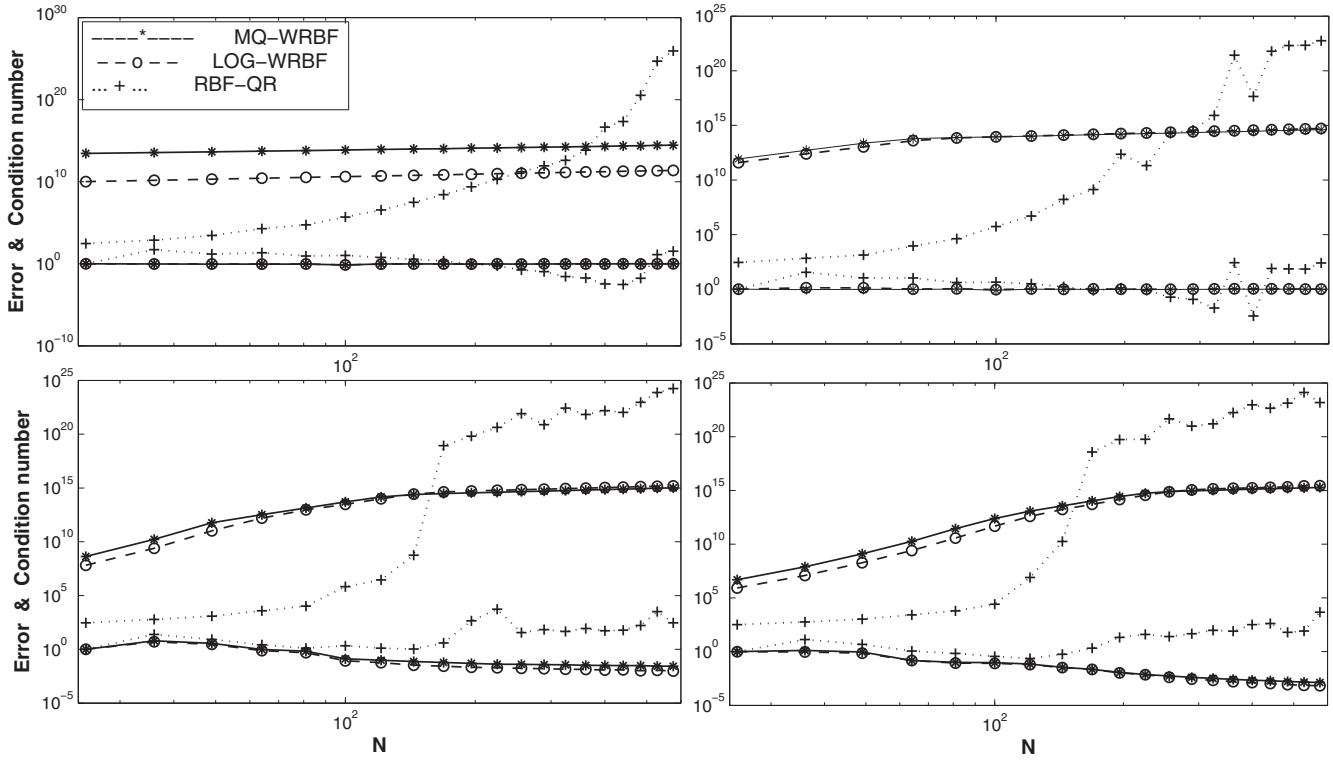

Fig. 15. The condition number and l_∞ error for solutions of 2d Poisson equation with exact solution w_3, with RBF-QR method, MQ-WRBF and LOG-WRBF basis with $\epsilon = 0.01$ (*up-right*) $\epsilon = 0.5$ (*up-left*) $\epsilon = 1$ (*down-right*) $\epsilon = 1.5$ (*down-left*) and $p = 10^{-12}$.

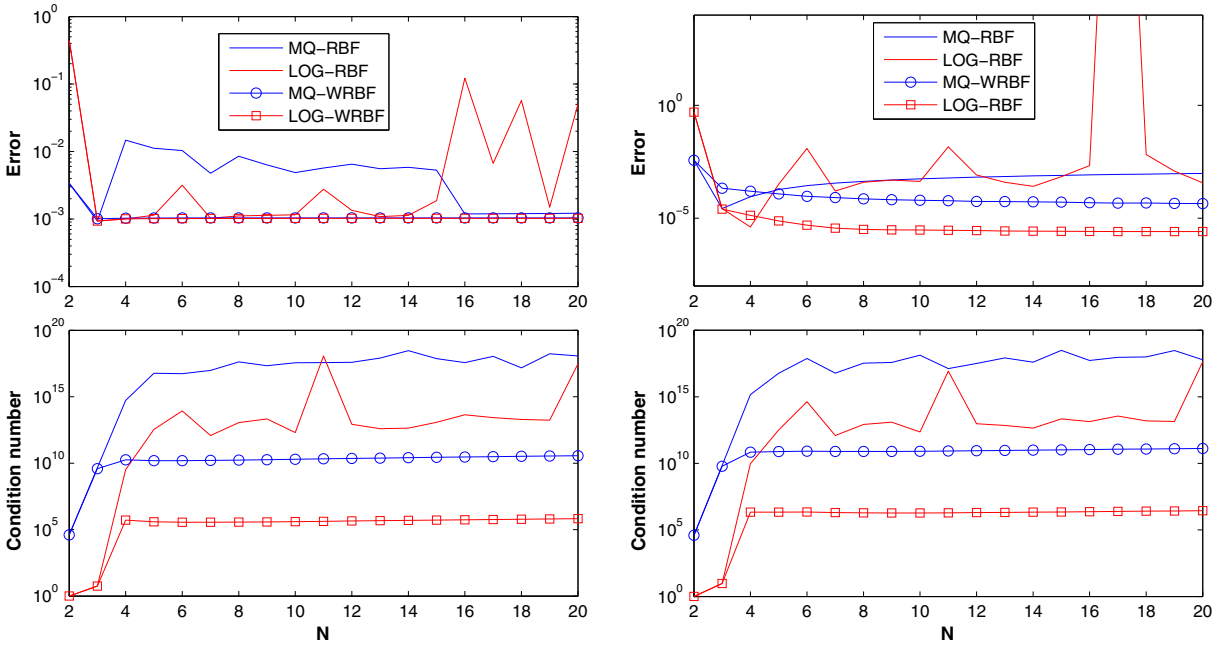

Fig. 16. The l_∞ error and condition number of $\tilde{\mathbf{C}}$ for WRBFs and standard RBFs with $\epsilon = 0.01$, $\Delta t = 1/100$, $p = 10^{-10}$ and $\beta = 0.5$ (*left*) and $\beta = 1$ (*right*).

Applying the Riemann-Liouville integral operator to both sides of (19) gives the following Volterra integral equation

$$u(x,t) = u(x,0) + \frac{1}{\Gamma(\beta)} \int_0^t (\gamma u_{xx}(x,\tau) + f(x,\tau))(t-\tau)^{\beta-1} d\tau. \qquad (20)$$

Discreatising this integral by a uniform time step and using the trapezoidal quadrature rule at time t_{k+1} yields

$$u(x,t_{k+1}) = u(x,0) + \frac{1}{\Gamma(\beta)} \int_0^{t_{k+1}} (\gamma u_{xx}(x,\tau) + f(x,\tau))(t-\tau)^{\beta-1} d\tau \qquad (21)$$

$$= u(x,0) + \frac{\Delta t^\beta}{\Gamma(\beta+2)} \sum_{j=0}^{k+1} a_{j,k+1} \big(\gamma u_{xx}(x,t_j) + f(x,t_j)\big), \qquad (22)$$

where

$$a_{j,k+1}=\begin{cases} k^{\beta+1}-(k-\beta)(k+1)^{\beta}, & j=0,\\ (k-j+2)^{\beta+1}-2(k-j+1)^{\beta+1}+(k-j)^{\beta+1}, & 1\leqslant j\leqslant k,\\ 1, & j=k+1. \end{cases} \tag{23}$$

By applying Kansa's method and using a uniform grid of any step of time, the problem converts to the following system of equations:

$$\tilde{\mathbf{C}}\mathbf{b}_{\mathbf{k+1}}=\tilde{\mathbf{d}}^{k+1}, \tag{24}$$

where

$$\tilde{\mathbf{C}}=\begin{bmatrix}\Psi^T(0)\\ \mathbf{C}\\ \Psi^T(L)\end{bmatrix},\qquad \tilde{\mathbf{d}}^{k+1}=\begin{bmatrix}u(0,t_{k+1})\\ \mathbf{d}^{k+1}\\ u(L,t_{k+1})\end{bmatrix},$$

$$\mathbf{d}_i^{k+1}=u(x_i,0)+sf(x_i,t_{k+1})+s\sum_{j=0}^{k}a_{j,k+1}h_j(x_i),$$

$$\mathbf{C}_{ij}=\psi_j(x_i)-s\gamma\psi_j''(x_i),\qquad i=2,\ldots,N-1,\quad j=1,\ldots,N,$$

and

$$s=\frac{\Delta t^{\beta}}{\Gamma(\beta+2)},\qquad h_k(x)=\gamma u_{xx}(x,t_k)+f(x,t_k).$$

At each step of time, the system (24) is solved for finding the unknown vectors $\mathbf{b}_{\mathbf{k+1}}$. It is noted that we only one time compute the Pseudo inverse of the matrix $\tilde{\mathbf{C}}$ by the Matlab command pinv($\tilde{\mathbf{C}}$).

The condition number of $\tilde{\mathbf{C}}$ and the l_∞ error for $\gamma=1$, $\beta=0.5$, $g(x)=65/(65+x^2)$, $\epsilon=0.01$ and final time are equal to 1, relevant to the WRBFs bases and standard RBFs presented in Fig. 16. This figure demonstrates that WRBFs can remove the instability arising from flat RBFs.

4. Conclusion

A special class of interpolation functions has been introduced. The structure of this class is based on adding the negative definite RBFs of order 1 to cardinal functions, and the advantages of this basis is, decreasing the condition number of the interpolation matrix while the convergence of the method remains similar to the RBFs methods. The new basis have a well-conditioned interpolation matrix whose condition number grows linearly with increasing N. Our method has been applied to four problems and numerical experiment corroborates our results. Therefore, the new basis overcomes the deficiencies of the flat RBFs, and we suggest it as an alternative for problems where these deficiencies prevent an accurate solution.

References

[1] A.E. Tarwater, A parameter study of Hardy's multiquadric method for scattered data interpolation, Report UCRL-53670, Lawrence Livermore National Laboratory, 1985.
[2] Franke R. Scattered data interpolation: test of some methods. Math. Comput. 1982;38:181–200.
[3] Kansa EJ. Multiquadrics-A scattered data approximation scheme with applications to computational fluid-dynamics-I surface approximations and partial derivative estimates. Comput. Math. Appl. 1990;19:127–45.
[4] Kansa EJ. Multiquadrics-a scattered data approximation scheme with applications to computational fluiddynamics- ii. Solutions to parabolic, hyperbolic and elliptic partial differential equations. Comput. Math. Appl. 1990;19:147–61.
[5] Boyd JP, McCauley PW. Quartic Gaussian and Inverse–quartic Gaussian radial basis functions: the importance of a nonnegative Fourier transform. Comput. Math. Appl. 2013;65:75–88.
[6] Buhmann MD. Radial Basis Functions: Theory and Implementations. New York: Cambridge University Press; 2004.
[7] Bustamante CA, Power H, Florez WF, Hang CY. The global approximate particular solution meshless method for two-dimensional linear elasticity problems. Int. J. Comput. Math. 2013;90:978–93.
[8] Wendland H. Scattered Data Approximation. New York: Cambridge University Press; 2005.
[9] Flyer N, Barnett GA, Wicker LJ. Enhancing finite differences with radial basis functions: experiments on the Navier-Stokes equations. J. Comput. Phys. 2016;316:39–62.
[10] Fornberg B, Zuev J. The Runge phenomenon and spatially variable shape parameters in RBF interpolation. Comput. Math. Appl. 2007;54:379–98.
[11] Fuselier EJ, Shankar V, Wright GB. A high-order radial basis function (RBF) Leray projection method for the solution of the incompressible unsteady Stokes equations. Comput. Fluids 2016;128:41–52.
[12] Heryudono A, Larsson E, Ramage A, von Sydow L. Preconditioning for radial basis function partition of unity methods. J. Sci. Comput. 2016;67:1089–109.
[13] Huber SE, Trummer MR. Radial basis functions for solving differential equations: Ill-conditioned matrices and numerical stability. Comput. Math. Appl. 2016;71:319–27.
[14] Lamichhane A, Chen C. Particular solutions of Laplace and bi-harmonic operators using Matern radial basis functions. Int. J. Comput. Math. 2017;94:690–706.
[15] Schaback R. Multivariate interpolation by polynomials and radial basis functions. Constr. Approx. 2005;21:293–317.
[16] Stevens D, Power H. The radial basis function finite collocation approach for capturing sharp fronts in time dependent advection problems. J. Comput. Phys. 2015;298:423–45.
[17] ul Islam S, Aziz I, Ahmad M. Numerical solution of two-dimensional elliptic PDEs with nonlocal boundary conditions. Comput. Math. Appl. 2015;69:180–205.
[18] Yun D, Hon Y. Improved localized radial basis function collocation method for multi-dimensional convection-dominated problems. Eng. Anal. Bound. Elem. 2016;67:63–80.
[19] Shivanian E. A meshless method based on radial basis and spline interpolation for 2-D and 3-D inhomogeneous biharmonic BVPs. Z. Naturforsch. A 2015;70:673–82.
[20] Hosseini VR, Shivanian E, Chen W. Local radial point interpolation (mlrpi) method for solving time fractional diffusion-wave equation with damping. J. Comput. Phys. 2016(312):307–32.
[21] Powell M. The Theory of Radial Basis Function Approximation in 1990. Oxford: Clarendon; 1992.
[22] Madych WR, Nelson SA. Multivariate interpolation and conditionally positive definite functions. Approx. Theory Appl. 1988;4:77–89.
[23] Sarra SA. Radial basis function approximation methods with extended precision floating point arithmetic. Eng. Anal. Bound. Elem. 2011;35:68–76.
[24] Fornberg B, Wright G. Stable computation of multiquadric interpolants for all values of the shape parameter. Comput. Math. Appl. 2004;48:853–67.
[25] Fornberg B, Piret C. A stable algorithm for flat radial basis functions on a sphere. SIAM J. Sci. Comp. 2007;30:60–80.
[26] Fornberg B, Larsson E, Flyer N. Stable computations with Gaussian radial basis functions. SIAM J. Sci. Comput. 2011;33:869–92.
[27] Larsson E, Lehto E, Heryudono A, Fornberg B. Stable computation of differentiation matrices and scattered node stencils based on gaussian radial basis functions. SIAM J. Sci. Comput. 2013;35:A2096–119.
[28] Wendland H, Rieger C. Approximate interpolation with applications to selecting smoothing parameters. Numer. Math. 2005;101:729–48.
[29] Sarra SA. Regularized symmetric positive definite matrix factorizations for linear systems arising from RBF interpolation and differentiation. Eng. Anal. Bound. Elem. 2014;44:76–86.
[30] Fasshauer GE. Meshfree Approximation Methods with MATLAB. Hackensack, NJ, USA: World Scientific Publishers; 2007.
[31] Beatson RK, Light WA, Billings S. Fast solution of the radial basis function interpolation equations: domain decomposition methods. SIAM J. Sci. Statist. Comput. 2001;22:1717–40.
[32] Sibson R, Stone G. Computation of thin-plate splines. SIAM J. Sci. Statist. Comput. 1991;12:1304–13.
[33] Narcowich FJ, Ward JD. Norms of inverses and condition for matrices associated with scattered data. J. Approx. Theory 1991;64:69–94.
[34] Pazouki M, Schaback R. Bases for kernel-based spaces. J. Comput. Appl. Math. 2011;236:575–88.
[35] Buhmann M, Dyn N. Spectral convergence of multiquadric interpolation. Numer. Math. 2005;101:729–48.
[36] Madych WR, Nelson SA. Bounds on multivariate polynomials and exponential error estimates for multiquadric interpolation. J. Approx. Theory 1992;70:94–114.
[37] Madych WR, Nelson SA. Error bounds for multiquadric interpolation. In: Approximation Therory VI. Academic Press; 1989. p. 413–6.
[38] Riley JD. Solving systems of linear equations with a positive definite, symmetric, but possibly ill-conditioned matrix. Math. Tables Other Aids Comput. 1955;9/51:96–101.
[39] Aslefallah M, Shivanian E. Nonlinear fractional integro-differential reaction-diffusion equation via radial basis functions. Eur. Phys. J. Plus 2015;130:47.

Dr. Saeed Kazem being first author did PhD in Applied Mathematics in 2017 from Amirkabir University of Technology, Iran.

Dr. Ali Hatam being corresponding author was a Lecturer in Applied Mathematics in 2005 from Amirkabir University of Technology, Iran and did PhD in Applied Mathematics in 2005 from University of Salford, UK.

Dr. Edmund A Chadwick begin third author was a Research Assistant in 1993 in Department of Marine Technology at University of Newcastle. He was a Research Associate in 1995 in Department of Engineering at University of Durham. He was a Hitachi Research Fellow in 1996 in Department of Mathematics at Trinity College (university), Dublin. He was a Senior Researcher in 1996 at Hitachi Research Laboratory, Trinity College (university), Dublin. He was a Senior Scientific Researcher in 1998 at BAESYST EMS ATC: Sowerby, Filton Bristol. He was a Lecturer grade A in 2000 from University of Salford. He was a Lecturer grade B in 2001 from University of Salford. He was a Senior Lecturer in 2008 from University of Salford. He was a Reader in Applied Mathematics in 2010 from University of Salford.